Available online at www.sciencedirect.com
SCIENCE DIRECT®
Chemical Physics Letters 395 (2004) 296–301
CHEMICAL PHYSICS LETTERS
www.elsevier.com/locate/cplett

Formation and kinetics study of cuprous oxide nanodots on $LaAlO_3$ (0 0 1)

Haitao Zhang, Duane M. Goodner, Michael J. Bedzyk, Tobin J. Marks [1], Robert P.H. Chang *

Department of Materials Science and Engineering and Materials Research Center, Northwestern University, Cook Hall, Room 2036, 2220 Campus Drive, Evanston, IL 60208, USA

Received 8 June 2004; in final form 8 June 2004
Available online 21 August 2004

Abstract

Cu_2O nanodots have been grown on $LaAlO_3$ (0 0 1) substrates using metalorganic chemical vapor deposition. X-ray diffraction reveals that the nanodots grow epitaxially on the substrate. The dots are hut-shaped islands with {1 1 1} side facets. Evolution of the nanodot shape, density, and size during growth has been analyzed by scanning electron microscopy and atomic force microscopy. It is shown that Ostwald ripening plays an important role in nanodot growth.

1. Introduction

Oxide semiconductors find extensive applications in photonic and electronic devices such as transistors, rectifiers, thin-layer capacitors, resistors, and thermistors. One important material among this class of oxides is Cu_2O, a p-type semiconductor with a direct band gap of ~2.17 eV [1,2]. The exceptionally long lifetime (tens of microseconds) of excitons in Cu_2O has made this material the focus of many efforts to observe Bose–Einstein Condensation (BEC) of excitons [3]. Nano-sized single-crystal Cu_2O is expected to exhibit spatially confined exciton states that will enhance the possibility of observing BEC. Low dimensional nanostructured materials are also subjects of much interest for their novel physical properties and potential device applications [4,5]. Cu_2O has also shown promise in solar cell applications due to its high absorption coefficient, non-toxicity, and low cost [6].

Recently, Cu_2O nanoparticles [1,7], nanocubes [8], and nanowires [9] have been synthesized using aqueous chemical methods. However, it is difficult to integrate nanostructures prepared by these techniques into actual devices. Three-dimensional (3D) island formation in the lattice mismatched heteroepitaxy provides a promising path for nanostructured device fabrication [4,5]. In recent years this growth mode has been extensively studied for various semiconductor systems including Ge/Si [10,11], InAs/GaAs [12], CdSe/ZnSe [13], and PbSe/PbTe [14], etc. However, relatively little work has been done on metal oxides, mainly due to the technical difficulties in preparing single crystal oxides with high perfection and purity. Cu_2O has a cuprite structure with only one isomorph being Ag_2O [15]. Lacking suitable substrate with similar structure makes the growth of Cu_2O more difficult. MgO (1 1 0) with a small (1.4%) lattice mismatch with Cu_2O was used as substrate for the formation of Cu_2O islands using metalorganic chemical vapor deposition (MOCVD). However the islands are multiple-shaped with a size of 300–500 nm [16]. It was reported that Cu_2O pyramid-shaped nanodots (NDs) can be formed on $SrTiO_3$ (0 0 1) substrate using

* Corresponding author. Fax: +1 847 491 4181.
E-mail address: r-chang@northwestern.edu (R.P.H. Chang).
[1] Also in Department of Chemistry, Northwestern University.

0009-2614/$ - see front matter © 2004 Elsevier B.V. All rights reserved.
doi:10.1016/j.cplett.2004.07.089

oxygen-plasma-assisted molecular beam epitaxy with a large lattice mismatch of 8.9% [17].

To form nano-sized Cu_2O islands with uniform shape, we chose $LaAlO_3$ (LAO) (0 0 1) as substrate for the growth of Cu_2O. LAO has a rhombohedral structure with the hexagonal cell parameters $a = 5.36$, $c = 13.10$ Å and $\alpha = 60.16°$ [18]. However, it can be also considered as a pseudo-perovskite structure with $a = 3.79$ Å, and $\alpha = 90.12°$ [19,20]. Compared to the lattice constant of Cu_2O (4.27 Å), LAO has a lattice mismatch of 12.7% with Cu_2O. This large lattice mismatch together with the large misfit in material chemistry is favorable for island growth, and also provides an opportunity to study the kinetics of island formation.

Using MOCVD growth techniques, we form hut-shaped Cu_2O NDs with ordered alignments on LAO (0 0 1) substrates. The epitaxial ND growth that occurs despite the large lattice mismatch between Cu_2O and $LaAlO_3$ was studied by X-ray diffraction (XRD). Scanning electron microscopy (SEM) and AFM were also used in the kinetics study of the effects of deposition parameters, such as deposition time, oxygen soak time, and growth temperature on the evolution of the Cu_2O ND size, area number density, and morphology.

2. Experimental

Cu_2O NDs were synthesized using the pulsed organometallic beam epitaxy system described elsewhere [21]. The LAO (0 0 1) substrates were ultrasonically cleaned in acetone and methanol, blown dry with nitrogen, and then introduced into the growth chamber where they were oxygen plasma-cleaned for about 1 h at 775–825 °C. During the subsequent ND growth, the O_2 partial pressure was held at approximately 2.7 m Torr. Purified Copper dipivaloylmethanate [$Cu(dpm)_2$] precursor vapor was pulsed into the reaction chamber through computer-operated valves used to control the duration of each pulse (pulse time, t_p), the separation time between each pulse (oxygen soak time, t_s), and the number of pulses (n_p) for the deposition. The total deposition time (t_d) is the number of pulses times the sum of the pulse time and the soak time [i.e., $t_d = n_p \times (t_p + t_s)$]. The Cu precursor flux during each pulse was about 10 Å/s as measured by a quartz crystal microbalance. Three series of samples were prepared to study the influence of n_p (Series A), t_s (Series B), and the substrate temperature (Series C) on ND growth. In each series, one of these parameters was varied while the other two remained constant. Details of the experimental parameters are listed in Table 1.

The as-synthesized samples were characterized using SEM (LEO 1525), XRD (Huber four-circle with Cu $K\alpha_1$ radiation from a Rigaku rotating anode with a graphite monochromator and 0.2° resolution), and AFM (Digital Instruments Nanoscope). Due to the very steep side facets of our Cu_2O NDs, standard silicon nitride AFM tips yield lateral broadening artifacts in the dot image due to convolution with tip size and shape. Thus, contact etched silicon probes with ultrasharp tips (nominal tip radius of 5–10 nm, and tip half angles of 17° side, 25° front and 10° back) and a very long cantilever length (450 μm) were used in the AFM measurement to lessen this convolution effect.

3. Results and discussion

Fig. 1 shows typical SEM images of a Cu_2O ND sample grown at 800 °C with a deposition time of 18 min (pulse time of 1 s, soak time of 8 s, and the number of pulses of 120). The collections of NDs in the image consist of both square-based and rectangular-based huts. Both types of huts have well-defined facets and the base edges of virtually all of the dots are oriented along the same set of in-plane orthogonal axes. As indicated in Fig. 1b, the substrate edge is along the LAO ⟨1 0 0⟩ direction, which was verified by the XRD ϕ-scan. Hence, the base edges of the NDs are determined to be aligned along two orthogonal ⟨1 1 0⟩ directions within the substrate (0 0 1) surface plane.

XRD studies were also used to study the crystallographic orientation of the NDs. Fig. 2a shows the results from an XRD θ–2θ (specular rod) scan performed on a Cu_2O ND sample. The only peaks present in this scan are the Cu_2O (0 0 2) and the LAO (0 0 l) (l = 1,2,3) reflections, indicating that the NDs are single-phase Cu_2O. The lattice parameter of 4.28 Å determined from the Cu_2O (0 0 2) peak position is close to the known Cu_2O bulk value of 4.267 Å indicating that most of the ND material is relaxed. A ω-rocking curve scan (inset of Fig. 2a), with a full width at half maximum (FWHM) of 0.40°, verifies that the dots are preferentially oriented with Cu_2O (0 0 1)‖LAO (0 0 1). Investigation of the off-normal Cu_2O {2 2 0} peaks by a 360°

Table 1
Parameters for three different series of Cu_2O nanodot growth experiments

Series	Deposition time, t_d (min)	Growth temperature (°C)	Pulse time, t_p (s)	Oxygen soak time, t_s (s)	Number of pulses, n_p
A	5.4–63	800	1	8	36–420
B	2–22	800	1	0–10	120
C	18	775–825	1	8	120

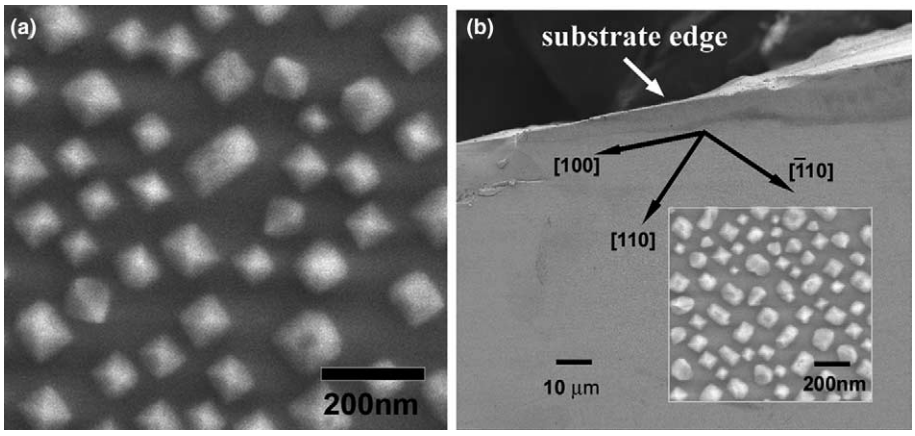

Fig. 1. (a) SEM image of Cu_2O nanodots on LAO (0 0 1); (b) SEM image shows the dot base edge orientations with respect to the substrate edge. Arrows show the edge orientations of the substrate and the dot bases. The background was taken under a low magnification, while the insect was zoomed in locally with a high magnification.

ϕ-scan (Fig. 2b) indicates an in-plane epitaxial relationship Cu_2O [1 0 0]‖LAO [1 0 0].

AFM measurement, combined with XRD and SEM results, was used to identify the facet orientations of Cu_2O NDs. The ND edge orientation along $\langle 1\,1\,0\rangle$ directions requires that the ND facet planes must be of the form $\{h\,h\,l\}$ where l cannot be zero, and the ridges between two adjacent facets are oriented along the $\langle 0\,h\,l\rangle$ directions. AFM measurements show that the side faces are inclined to the substrate (0 0 1) surface with an average angle of 50° ± 2°. An average angle of 44.1° ± 0.7° between the $\langle 0\,h\,l\rangle$ oriented ridges and the (0 0 1) surface is also revealed by the AFM measurements. Due to the AFM tip convolution effect, the measured values of these angles are artifactually smaller than the actual values. Thus, the $\{h\,h\,l\}$ planes in closest agreement with these experimental results are the {1 1 1} planes, which have an angle of 54.7° with respect to the (0 0 1) plane, and $\langle 0\,1\,1\rangle$ oriented ridges with an angle of 45° to the (0 0 1) surface. It can therefore be concluded that the facets of the Cu_2O NDs are {1 1 1} planes. The {1 1 1} Cu_2O surface is expected to have a lower surface energy than the 1 0 0 surface because the {1 1 1} surface is nonpolar while the {1 0 0} surface is polar. Polar surfaces are not stable due to the long range Coulomb interaction which tends to drive the formation of nonpolar surfaces [22]. These side facets are extremely steep with respect to the epitaxial surface. A similar situation was also found in the growth of PbSe dots on PbTe (1 1 1) substrates where the side facets were {1 0 0} oriented [14].

The fact that most of the volume of Cu_2O ND material on the LAO substrates is completely relaxed indicates that the growth of Cu_2O NDs is different from coherent 3D island formation for heteroepitaxial systems such as Ge/Si [10,11], and InAs/GaAs [12]. Similar phenomena have been observed in PbSe/PbTe (5.5% tensile strain) [14] and InN/GaN (10% compressive strain) [23,24] systems. In situ reflection high energy electron diffraction studies showed that in the PbSe/PbTe system, the strain energy only accumulated during

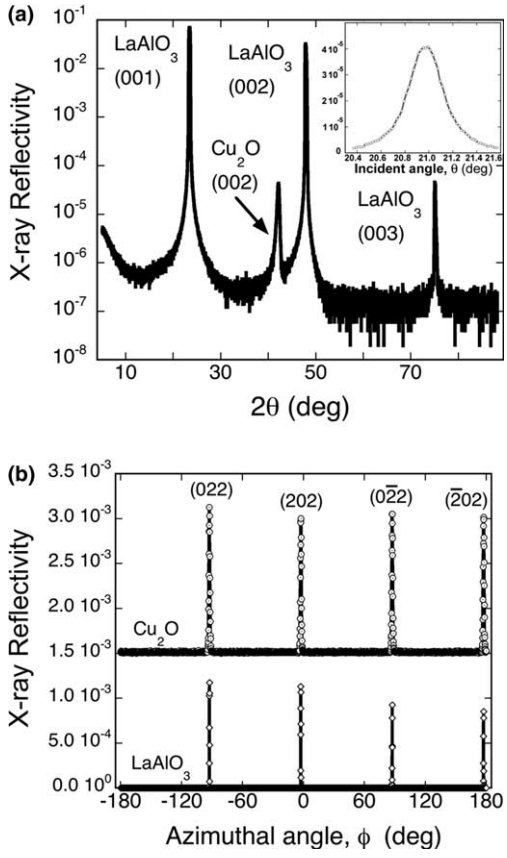

Fig. 2. XRD of Cu_2O nanodots on LAO (0 0 1): (a) θ-2θ scan along LAO (0 0 1) specular rod; (b) ϕ-scan through Cu_2O {0 2 2} and LAO {0 2 2} peaks (Cu_2O data are magnified by 200× and offset by 1.5×10^{-3}). Inset is a Cu_2O (0 0 2) rocking curve with a FWHM of 0.40°.

Table 2
Cu_2O nanodot densities and sizes with deposition times varying from 5.4 to 63 min

Deposition time, t_d (min)	Average height, h_a (nm)	Area density, n (μm^{-2})	Average base size, d_a (nm)	Width of base size distribution, w (nm)
5.4	21	123	36	8
18	46	52	96	21
45	81	22	152	37
63	93	9	68	42
		6	233	243

the first few monolayers of growth, and relaxed rapidly through islanding [14]; while in the InN/GaN system, most of the strain energy relaxed through the formation of dislocated islands on the surface [24]. With a large (12.7%) misfit in compression, the strain for Cu_2O NDs on LAO(0 0 1) may also relaxed mostly through the formation of dislocated islands on the surface. However, due to the lack of in situ measuring techniques for our MOCVD system, this needs to be proved by further investigation of the interface structure.

Samples in series A were prepared with deposition times of 5.4, 18, 45 and 63 min. Changes in the dot size and dot density with increasing deposition time are summarized in Table 2. The average height of the dots was measured by AFM, and other data were from SEM images analyzed using the software of analySIS (Soft Imaging System GmbH). The dot density n is the area number density of the dots. The average dot base size d_a and the width of the size distribution w were determined from the Gaussian fits of dot base mean diameter histograms. Typical AFM images, SEM images, and base size histograms of Cu_2O ND samples with deposition times of 18 and 63 min are shown in Fig. 3. Close-up SEM and AFM images (insets of Figs. 3b and d) of NDs prepared using $T_d = 63$ min show new facets that have begun to grow, and effectively rounded off the ridges between two adjacent pre-existing facets. Some of the NDs also become flat-topped (inset of Fig. 3d). Formation of these additional facets is driven by the high surface energies of the relatively sharp ridges (with small radii of curvature) formed during the early stages of dot growth.

The data in Table 2 show that as T_d increases the average dot size and the width of the dot size distribution both increase, while the dot density decreases. During the early stages of growth the dot size distribution can be modeled using a single Gaussian function (Fig. 1e), but after a sufficiently long deposition time, the dot size distribution becomes bimodal (Fig. 1f). These phenomena clearly indicate that an Ostwald ripening process accompanies the Cu_2O ND growth. Ripening process originates from the kinetic limitation in term of low adatom mobility or high deposition rate. In our experiment, a substrate growth temperature as high as about 800 °C was used to permit high adatom mobility during ND growth. However, the adatom mobility at

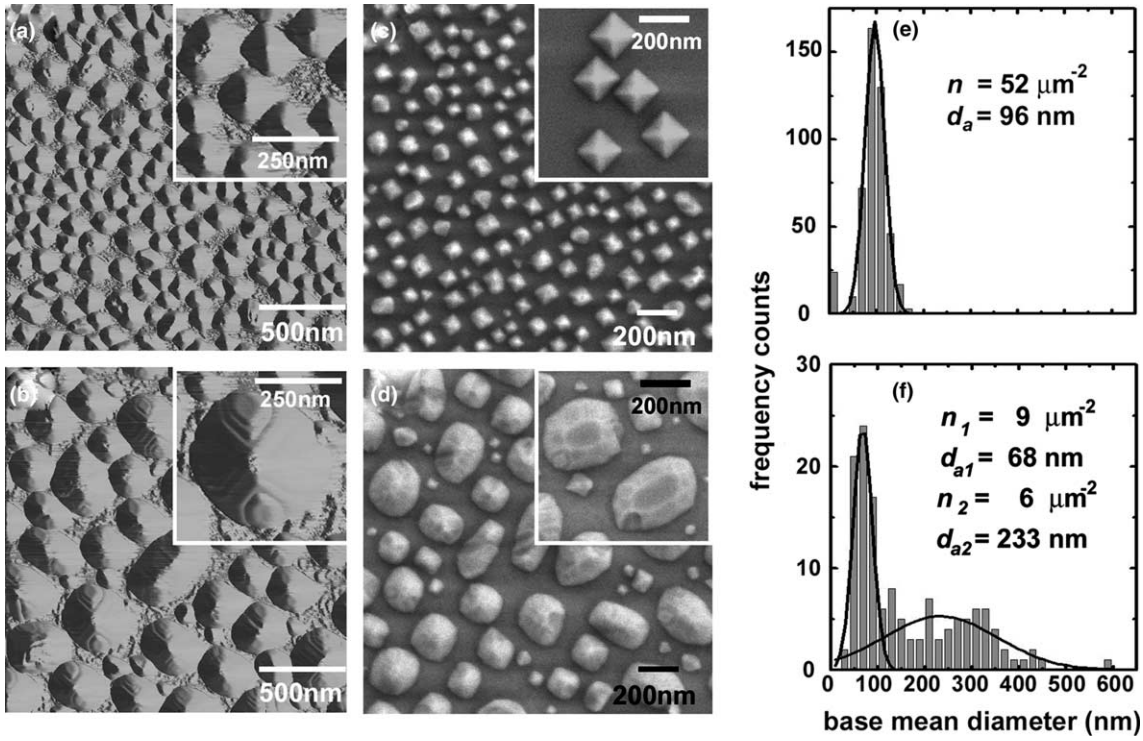

Fig. 3. Left: AFM images of Cu_2O nanodots with deposition times of: (a) 18 min (b) 63 min. Middle: Corresponding SEM images. Right: Corresponding dot base mean diameter histograms with Gaussian fits indicated by solid lines.

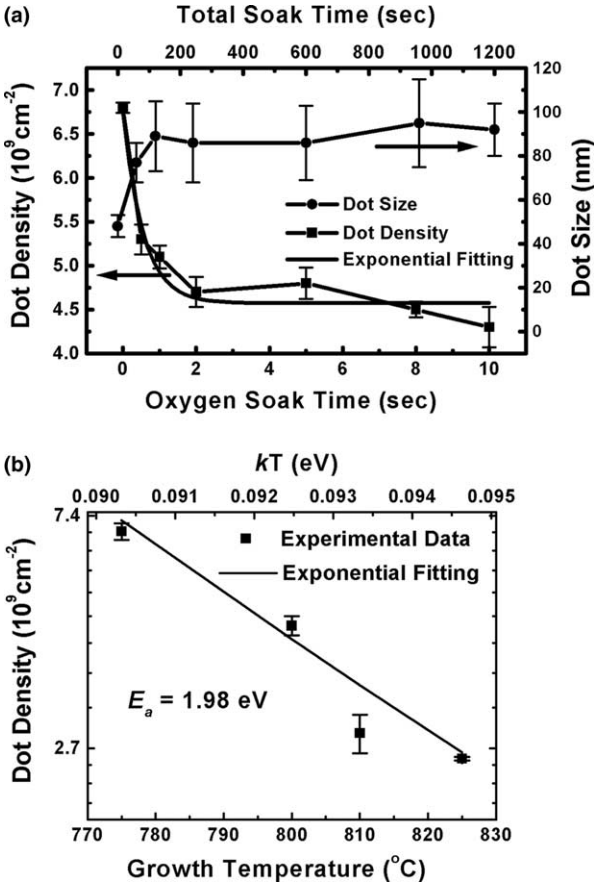

Fig. 4. (a) Cu_2O nanodot density and dot size (average dot base size) vs. oxygen soak time. The error bars of dot size indicate the widths of the dot size distributions; (b) Dot density vs. growth temperature. The exponential fit gives an activation energy of 1.98 eV.

this temperature is still too low to accommodate the ~10 Å/s precursor flux that impinges on the substrate during each pulse within the pulse time alone.

Experiments of series B and C were carried out to study the ripening effect on the ND growth. In experiment series B, dot evolution was investigated with the increase of oxygen soak time. A constant material coverage was kept in the experiment by keeping the pulse time and the number of pulses constant as 1 s and 120 pulses, respectively. So this experiment is equivalent to an annealing experiment. Fig. 4a shows how the experimentally measured dot density and the average dot base size on samples in series B varies as a function of oxygen soak time. These results reveal an exponential decrease in dot density and increase in average dot base size toward steady values as soak time increases. The exponential decay fit in Fig. 4a yields a time constant of 0.5 s. Fig. 4b shows the dot densities measured on series C samples prepared using different substrate temperatures but identical soak times and numbers of pulses during ND growth. These results show that as the growth temperature is increased, the dot density decreases. An exponential fit to these data gives an activation energy of 1.98 eV. As suggested by Kamins et al. [25] the steady dot distribution in annealing experiment may be due to: (1) Ostwald ripening restrained by an attachment barrier that increase with increasing island size; or (2) a steady-state distribution determined by chemical equilibrium. Since the strain-free Cu_2O NDs may be grown via forming dislocated islands on the surface, an equilibrium distribution may not be expected here compared to the island growth with a coherent Stranski–Krastanov mode. The steady distribution under a long oxygen soak time should result from a restrained Ostwald ripening by an attachment/detachment barrier. And the large activation energy of 1.98 eV may mainly result from the adatom attachment/detachment barrier for these highly faceted Cu_2O NDs.

4. Conclusions

We have demonstrated the growth of Cu_2O NDs on LAO (0 0 1) substrates using MOCVD. The dots are square-based and rectangular-based huts exhibiting facets determined to be {1 1 1} faces based on SEM and AFM measurements. XRD analysis indicates ordered Cu_2O NDs can be epitaxially grown on LAO (0 0 1) substrates despite the large lattice mismatch of 12.7% between Cu_2O and LAO. The Cu_2O NDs may be formed through the formation of dislocated islands on the surface. Observations of the evolution of ND size and number density indicate that Ostwald ripening also plays an important role in ND growth. This work shows that oxides may provide another example for the studying of the growth mechanism of heterostructres in addition to the widely studied conventional semiconductors.

Acknowledgements

This work has been supported by the NSF (CHE-0201767 and DMR 0076097). The authors acknowledge use of the Northwestern MRSEC central facilities.

References

[1] K. Borgohain, N. Murase, S. Mahamuni, J. Appl. Phys. 92 (2002) 1292.
[2] J.A. Switzer, C.J. Hung, L.Y. Huang, E.R. Switzer, D.R. Kammler, T.D. Golden, E.W. Bohannan, J. Am. Chem. Soc. 120 (1998) 3530.
[3] D. Snoke, Science 298 (2002) 1368.
[4] P.M. Petroff, G. Medeiros-Ribeiro, MRS Bull. 21 (1996) 50.
[5] N.N. Ledentsov, V.M. Ustinov, V.A. Shchukin, P.S. Kop'ev, Z.I. Alferov, D. Bimberg, Semiconductors 32 (1998) 343.

[6] S.O. Ishizuka, S. Kato, T. Maruyama, K. Akimoto, Jpn. J. Appl. Phys. Part 1 40 (2001) 2765.
[7] Y.J. Dong, Y.D. Li, C. Wang, A.L. Cui, Z.X. Deng, J. Colloid Interf. Sci. 243 (2001) 85.
[8] L.F. Gou, C.J. Murphy, Nano Lett. 3 (2003) 231.
[9] W.Z. Wang, G.H. Wang, X.S. Wang, Y.J. Zhan, Y.K. Liu, C.L. Zheng, Adv. Mater. 14 (2002) 67.
[10] Y.W. Mo, D.E. Savage, B.S. Swartzentruber, M.G. Lagally, Phys. Rev. Lett. 65 (1990) 1020.
[11] D.J. Eaglesham, M. Cerullo, Phys. Rev. Lett. 64 (1990) 1943.
[12] D. Leonard, K. Pond, P.M. Petroff, Phys. Rev. B 50 (1994) 11687.
[13] S. Lee, I. Daruka, C.S. Kim, A.L. Barabasi, J.L. Merz, J.K. Furdyna, Phys. Rev. Lett. 81 (1998) 3479.
[14] M. Pinczolits, G. Springholz, G. Bauer, Appl. Phys. Lett. 73 (1998) 250.
[15] P.R. Markworth, R.P.H. Chang, Y. Sun, G.K. Wong, J.B. Ketterson, J. Mater. Res. 16 (2001) 914.
[16] P.R. Markworth, X. Liu, J.Y. Dai, W. Fan, T.J. Marks, R.P.H. Chang, J. Mater. Res. 16 (2001) 2408.
[17] Y. Liang, A.S. Lea, D.E. McCready, P. Meethunkij, Electrochem. Soc. Proc. 2001-5 (State-of-the-Art Application of Surface and Interface Analysis Methods to Environmental Material Interactions) (2001) 125.
[18] E. Taspinar, A.C. Tas, J. Am. Ceram. Soc. 80 (1997) 133.
[19] H. Lehnert, H. Boysen, J. Schneider, F. Frey, D. Hohlwein, P. Radaelli, H. Ehrenberg, Z. Kristallogr. 215 (2000) 536.
[20] H. Lehnert, H. Boysen, P. Dreier, Y. Yu, Z. Kristallogr. 215 (2000) 145.
[21] S.J. Duray, D.B. Buchholz, S.N. Song, D.S. Richeson, J.B. Ketterson, T.J. Marks, R.P.H. Chang, Appl. Phys. Lett. 59 (1991) 1503.
[22] S.J. Chen, X.T. Chen, Z.L. Xue, L.H. Li, X.Z. You, J. Cryst. Growth 246 (2002) 169.
[23] O. Briot, B. Maleyre, S. Ruffenach, Appl. Phys. Lett. 83 (2003) 2919.
[24] G. Feuillet, B. Daudin, F. Widmann, J.L. Rouviere, M. Arlery, J. Cryst. Growth 190 (1998) 142.
[25] T.I. Kamins, G. Medeiros-Ribeiro, D.A.A. Ohlberg, R.S. Williams, J. Appl. Phys. 85 (1999) 1159.